Journal of Catalysis **184,** 112–122 (1999)
Article ID jcat.1999.2442, available online at http://www.idealibrary.com on IDEAL®

Reversible Catalyst Deactivation in the Photocatalytic Oxidation of Dilute *o*-Xylene in Air

M. Mahbub Ameen and Gregory B. Raupp[1]

Department of Chemical, Bio., and Materials Engineering, Arizona State University, Tempe, Arizona 85287-6006

Received September 1, 1998; revised January 8, 1999; accepted January 11, 1999

The reversible deactivation rate during gas–solid heterogeneous photocatalytic oxidation of airborne dilute *o*-xylene over near-ultraviolet irradiated titanium dioxide catalyst depends on *o*-xylene concentration and the relative humidity of the reactant stream. Deactivation kinetics can be described by an exponentially decaying deactivation factor with time on stream. The exponential deactivation factor α decreases linearly with decreasing *o*-xylene concentration and increasing relative humidity. The catalyst can be completely regenerated by passing humid air through the bed under continuous UV-irradiation, showing that the deactivation process is reversible. Infrared spectroscopy during UV irradiation and continuous flow of *o*-xylene-contaminated air indicates adsorption of *o*-xylene, along with formation of *o*-tolualdehyde, *o*-toluic acid, and benzoate ion. Infrared bands of the complete oxidation product carbon dioxide are also observed. The titania surface coverages of the reactant and aromatic partial oxidation intermediates are significantly higher for conditions of low relative humidity than for conditions of high humidity. Experiments performed at low relative humidity favor the buildup of *o*-xylene and *o*-toluic acid on the catalyst surface, and these species may be responsible for the apparent loss in activity. Regeneration of the catalyst deactivated during the photocatalytic oxidation process run at high humidity requires much shorter catalyst treatment time than that for the catalyst deactivated by photocatalytic oxidation run at low humidity. This phenomenological behavior suggests that hydroxyl radicals play a significant role in both the oxidation and the regeneration processes.

INTRODUCTION

Deactivation of the titanium dioxide catalyst during gas–solid photocatalytic oxidation (PCO) of air (1–20) contaminated by select classes of chemical compounds is a serious issue and deserves attention from both commercializers of the technology and academic researchers. Included among these troublesome compounds are alcohols (15, 16), aromatics (17–20), and those containing Si or N heteroatoms (14). Based on the available evidence, it appears that the mode of deactivation is dependent on chemical compound class. Blake and Griffin (16) used infrared spectroscopy to identify surface adsorbed carboxylate species during butanol PCO and suggested that this nonvolatile partial oxidation byproduct accumulated on the catalyst surface and blocked the active sites. Aromatics such as benzene and chlorobenzene convert with low photoefficiency and tend to deactivate the catalyst through buildup of carbonaceous residue on the surface (17), likely in the form of recalcitrant aromatic compounds. Jacoby *et al*. (18) observed gradual reversible deactivation of the catalyst during PCO of benzene. Only carbon dioxide and small concentrations of carbon monoxide were detected in the gas phase. In an attempt to identify the adsorbed species, water was used as a solvent to extract the adsorbed species from the catalyst surface and the solution was analyzed by HPLC. The adsorbed intermediates were identified as phenol, benzoquinone and/or hydroquinone, and malonic acid. The catalyst could be fully regenerated by flowing zero grade air in the presence of UV light for several hours.

Toluene and *m*-xylene photocatalytic oxidation in a single pass catalyst powder bed has been reported recently (19, 20). No volatile intermediates were detected by gas chromatography in either case. However, Luo and Ollis (20) observed catalyst deactivation with each toluene run. Benzoic acid was identified as one of the adsorbed species by GC/MS analysis of a methanol solution that was used to extract adsorbed species from the catalyst. In a subsequent study, Sauer *et al*. (19) observed that the photocatalytic oxidation of dilute mixtures of toluene and 1,1,3-trichloropropene (TCP) or perchloroethylene (PCE) in air increased the toluene conversion to 100% from the pseudosteady single component toluene feed conversion levels of 10–20%. However, catalyst deactivation was observed with all runs that contained toluene in the feed.

Peral and Ollis (14) studied PCO of decamethyltetrasiloxane (DMTS), pyrrole, indole and dimethyl sulfide, and observed that deactivation occurred for all these compounds except dimethyl sulfide. Auger spectroscopy showed that silicon from the DMTS and nitrogen from the pyrrole or indole deposited irreversibly on the catalyst

[1] To whom correspondence should be addressed. Fax: (602) 965-0037. E-mail: raupp@asu.edu.

0021-9517/99 $30.00

surface. Carbon was also deposited in an unidentified nonvolatile form. Neither sulfur nor carbon was deposited on the catalyst when dimethyl sulfide was photocatalytically oxidized. In our laboratory, we have observed rapid deactivation of the catalyst during PCO of hexamethyl disilazane (HMDS), a silicon-containing compound (21). In this case, the HMDS reacted with the hydroxylated titania to produce a surface layer of inert methyl silyl groups.

In this study we investigate the reversible deactivation of UV-irradiated titanium dioxide during photocatalytic oxidation of *o*-xylene. Powder-bed conversion experiments were performed to empirically quantify the deactivation kinetics. *In situ* infrared experiments were performed in a continuous flow environment to identify the adsorbed species that build up on the catalyst surface during deactivation and to track the destruction of these nonvolatile intermediates during photocatalyst regeneration.

EXPERIMENTAL METHODS

Powder Bed Experiments

Deactivation kinetics studies were carried out in a powder-bed microreactor (1) using a gas flow and analysis apparatus described in detail elsewhere (10). A Varian 3700 series gas chromatograph equipped with an FID detector for volatile organic compound analysis and a methanizer/FID for CO_2 analysis, along with an in-line CO sensor were used to analyze the air stream. The catalyst was P25 (Degussa) with primary diameter of 30 nm, a surface area of 50 ± 15 m^2/g, and crystal structure of primarily anatase. The powdered semiconductor was used as supplied without pretreatment. The diameter and thickness of the catalyst bed were 16 and 1 mm, respectively. The mean gas residence time in the catalyst bed was 0.22 s. A 4-W fluorescent "black light" bulb (General Electric, F4TW-BLB) was used to irradiate the catalyst surface; the UV intensity on the catalyst surface was $\sim 5.5 \times 10^{-9}$ Einstein/cm^2-s (1.8 mW/cm^2) as measured by a Minolta integrating UV photometer. Differential conversion (<12%) was maintained for all experimental runs.

In Situ Infrared Experiments

The *in situ* infrared experiments were performed using a custom made photoreactor (infrared cell). A detailed description of this photoreactor and the flow assembly can be found elsewhere (22). Transmission infrared spectra of the catalyst surface were collected using a Nicolet 60SX Fourier transform infrared (FTIR) instrument using a photoconductive infrared detector with liquid nitrogen-cooled HgCdTe element. A thin coating of titania on a Si substrate was employed as the catalyst. The catalyst was prepared by dip-coating a double-side polished wafer in a slurry of Degussa P25 titania, followed by low-temperature drying. Film thickness was approximately 6 μm. All infrared experiments were performed with an air stream containing 50 ppm$_v$ *o*-xylene and a mean gas residence time of 2 s in the reactor. The UV flux to the substrate was held constant at approximately 4.6×10^{-9} Einstein/cm^2-s (1.5 mW/cm^2).

RESULTS

Powder Bed Experiments

Fixed powder bed deactivation experiments were run following the equilibrium adsorption of *o*-xylene under flowing conditions in the absence of UV. It took approximately 2 to 4 h to attain equilibrium depending upon the relative humidity and *o*-xylene concentration. Following the equilibration step, the UV lamp was illuminated to irradiate the catalyst surface and the product gases were analyzed at regular intervals. The *o*-xylene concentration in the reactor effluent dropped soon after the catalyst bed was irradiated with UV, indicating *o*-xylene destruction by photocatalytic oxidation. Within a limited process window of low *o*-xylene concentration and high humidity, steady state conversion was achieved and could be maintained for more than 12 h on stream. More commonly, *o*-xylene conversion decreased with increasing time on stream, indicating deactivation of the catalyst. The catalyst typically turned yellowish after being on stream for 2–3 h under these conditions. It appeared that the rate of deactivation depended on water vapor and *o*-xylene concentration. The effect of these parameters on deactivation is described below.

Effect of humidity. Figure 1 shows the time evolution of the *o*-xylene destruction rate over the course of the first 2 h on stream as a function of the relative humidity (RH) of the reactant stream for a fixed *o*-xylene concentration level of 25 ppm$_v$. The deactivation rate increases as the concentration of the water vapor in the inlet stream decreases. For RH less than or equal to 70%, deactivation continued with continuing time on stream until the catalyst was essentially completely deactivated after about 6 h total reaction time. In contrast, for RH above 80%, short-term deactivation ceased after about 2 h on stream and activity remained constant thereafter up to 12 h on stream. For air streams with relative humidity above 80%, the *o*-xylene conversion level was fairly constant, indicating very little or no deactivation.

To quantify the deactivation rate, the apparent reaction rate versus time data over the first 2 h of each run were fit with a simple empirical exponential model;

$$\text{apparent rate} = \Phi \cdot \text{intrinsic rate}$$
$$\Phi = \exp(-\alpha t),$$

where the intrinsic rate is the reaction rate in the absence of deactivation, Φ is the deactivation parameter, t is the

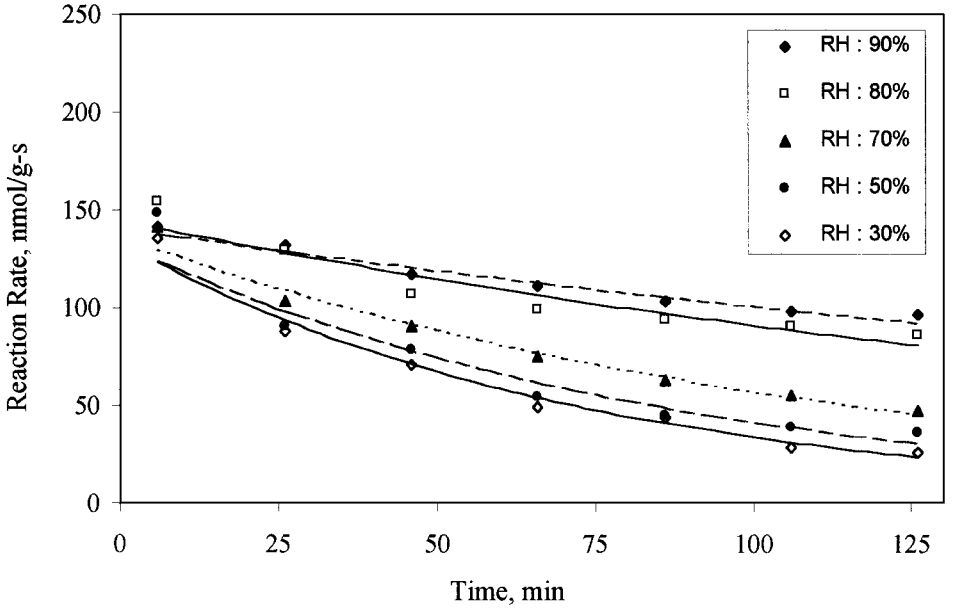

FIG. 1. Photocatalytic oxidation rate versus time as a function of relative humidity. *o*-xylene concentration fixed at 25 ppm_v.

time on stream, and α is a deactivation rate parameter. The curves (solid lines) shown in Fig. 1 represent the best fit to each individual condition using this exponential functionality through adjustment of the empirical deactivation rate parameter at each RH condition. The dependence of the extracted α values on relative humidity is shown in Fig. 2. The data can be reasonably fit by a straight line with slope equal to $-0.0002\ s^{-1}$.

Effect of concentration. Figure 3 shows the *o*-xylene disappearance rate versus time as a function of *o*-xylene feed concentration with relative humidity fixed at a value of 80%. With 75 ppm_v of *o*-xylene in the feed, deactivation is quite rapid. The deactivation rate decreases as the concentration of the contaminant is lowered. Note that the initial reaction rate (short time values) increases with increasing *o*-xylene concentration. For the 50 and 75 ppm_v runs, deactivation continued with continuing time on stream. In contrast, steady state conversion was achieved in the 25 ppm_v experiment after 2 h on stream as evidenced by a constant reaction rate of 90 ± 3 nmol/g-s. This rate was maintained for the entire 12-h duration of the test.

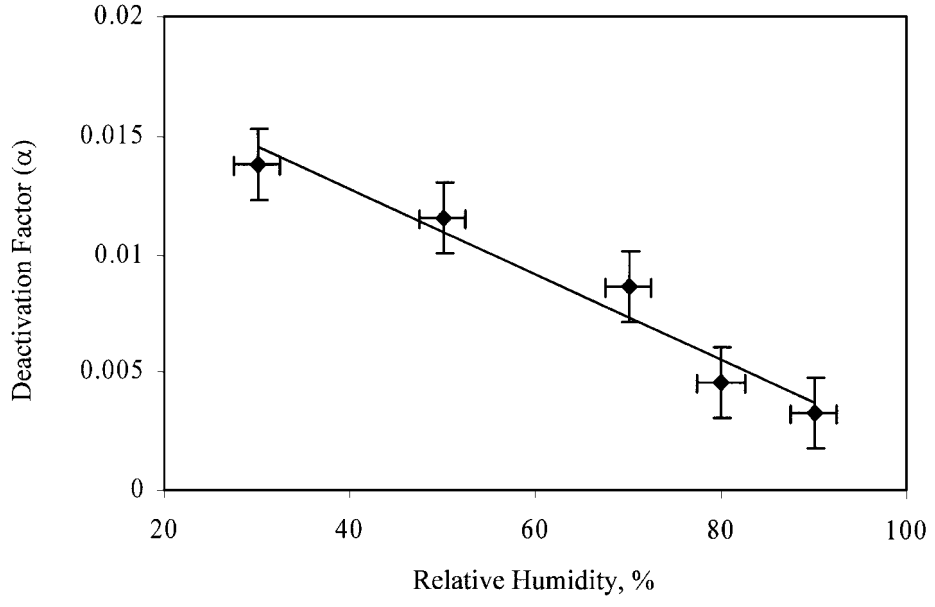

FIG. 2. Deactivation factor α versus relative humidity. *o*-xylene concentration fixed at 25 ppm_v.

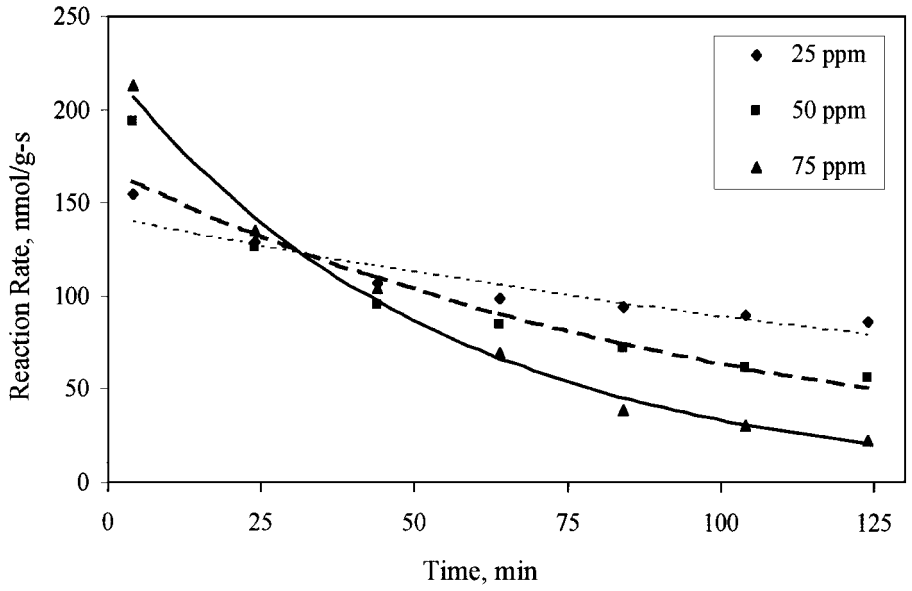

FIG. 3. Photocatalytic oxidation rate versus time as a function of *o*-xylene concentration. Relative humidity fixed at 80%.

The data are well described by the exponential deactivation function described above. Figure 4 shows the dependence of the deactivation rate parameter α on *o*-xylene concentration. As shown in the figure, the observed dependence can be approximated (correlation coefficient of 0.93) with a straight line of slope equal to $+0.0002$ ppmv^{-1} s^{-1}. Visually, it appears that there may exist some nonlinearity in the deactivation factor concentration dependence. In fact a power law dependence with an exponent of approximately 1.3 provides a substantially better statistical fit (correlation coefficient greater than 0.98). Verification of the suggested nonlinear dependence awaits further experimentation.

Catalyst regeneration. Catalyst deactivation could be reversed by regenerating the used catalyst by flowing humid, zero-grade air through the bed with continuous UV irradiation. The effect of a 12-h regeneration run on subsequent catalyst activity is shown in Fig. 5. The figure compares the time evolution of photocatalyst activity for two experiments run under identical conditions (25 ppm$_v$ *o*-xylene, 80% relative humidity), with one experiment run

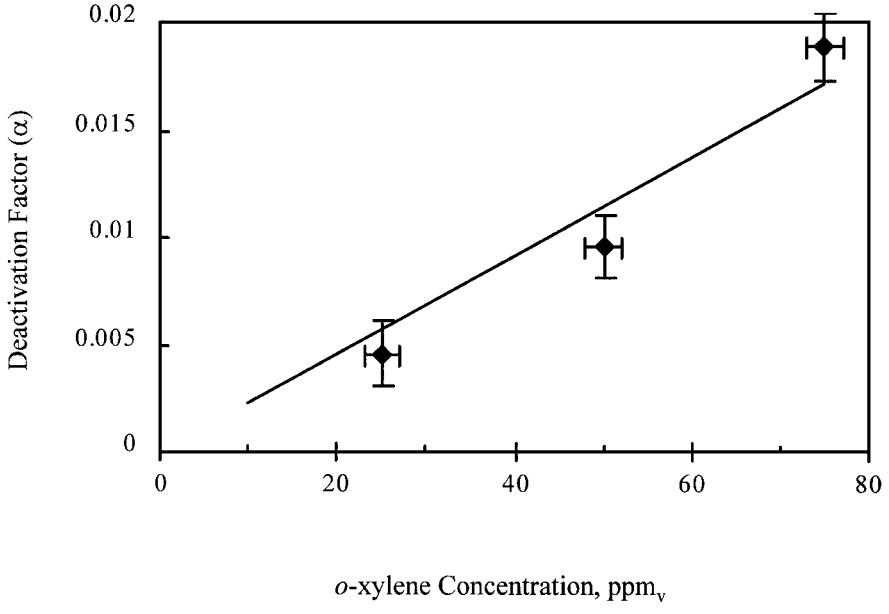

FIG. 4. Deactivation factor α versus *o*-xylene concentration. Relative humidity fixed at 80%.

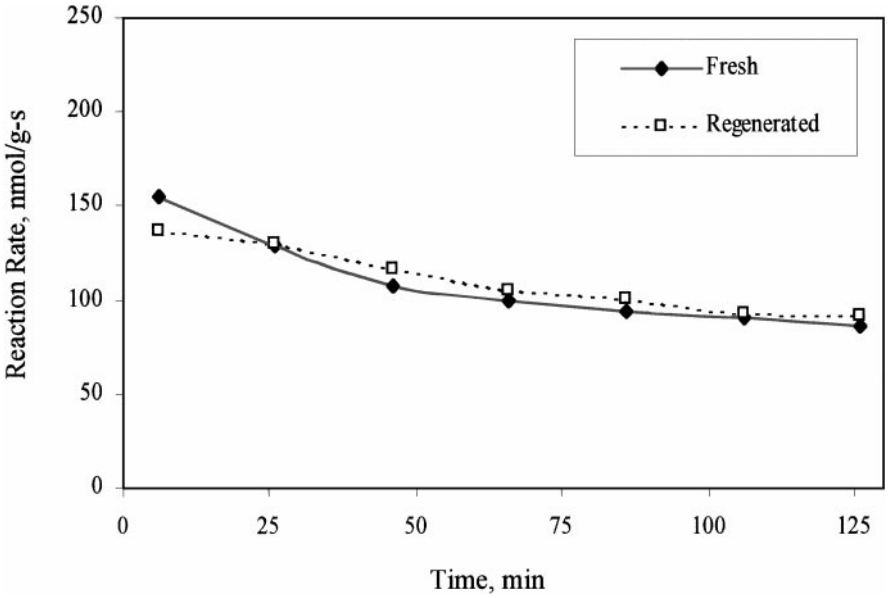

FIG. 5. Photocatalytic oxidation rate versus time with fresh and regenerated catalyst. *o*-Xylene concentration equal to 25 ppm_v; relative humidity equal to 80%.

using fresh catalyst and the other experiment using the regenerated catalyst. The fresh and regenerated catalysts exhibit nearly identical behavior. The deactivated catalyst regained its full activity after regeneration, demonstrating that the deactivation is a reversible process for this particular system. During regeneration, gas chromatographic analysis did not detect the presence of *o*-xylene or any other organic contaminant in the regenerating humid air effluent from the reactor, nor was CO detected. Instead, only carbon dioxide was evolved from the catalyst surface.

Infrared Spectroscopy during Photocatalytic Oxidation

The objective of the infrared experiments was to identify the adsorbed reactants, intermediates and products adsorbed on the catalyst surface during deactivation and regeneration. In general, such information provides vital understanding of the governing processes and can play an important role in the development of mechanistically based rate expressions. Deactivation results are described here; regeneration is described in the next subsection.

The time evolution of the infrared bands during PCO of *o*-xylene is shown in Fig. 6. Spectra were collected at 15-min intervals from the start of irradiation. The experiment was conducted with an RH equal to 20%. All spectra are ratioed to the spectrum of titanium dioxide in pure air with 20% relative humidity. The mean residence time in the photoreactor was 2 s. Note that due to total gas flow rate limitations, a much higher residence time is employed in infrared experiments than in powder-bed experiments. The spectrum of the catalyst surface in equilibrium with flowing air contaminated with *o*-xylene flow shown in Fig. 6a does not exhibit any detectable infrared absorption bands. Figures 6b through 6e show time-averaged spectra of the catalyst during UV irradiation for the following times on stream: 0–15, 15–30, 30–45, and 45–60 min, respectively. Figures 6f and 6g are time-averaged spectra of the catalyst surface for 105–120 min and 165–180 min on stream, respectively. Most of the spectral changes occur over the first 2 h of UV irradiation; although the bands continue to develop after that time frame, they do so at a much reduced rate. Because the differences between the spectra in Figs. 6f and 6g were not significant, the experiment was terminated at the end of 3 h on steam.

The development of major new bands is initiated by UV irradiation. To clarify the qualitative and quantitative nature of the time-evolution of the infrared spectra, peak intensities were tracked as a function of time and are plotted in Fig. 7. These derived data reveal different temporal trends for different bands. This knowledge facilitates grouping of band assignments to common surface-bound reaction intermediates or identifying different bands as those associated with different intermediates. Table 1 summarizes the major band assignments that are rationalized in the following text. Confirmation of these assignments awaits further investigation (e.g., dark experiments using internal reflection spectroscopy and isotope labeling studies).

The bands at 2361 and 2341 cm^{-1} are due to gas phase and adsorbed carbon dioxide (4) produced as a consequence of complete oxidation of *o*-xylene. These bands decrease with increasing time on stream as expected for a catalyst experiencing deactivation. The broad upward peak at ~3450 corresponds to the hydrogen bonded water and associated hydroxyls (4), whereas the sharp upward peak

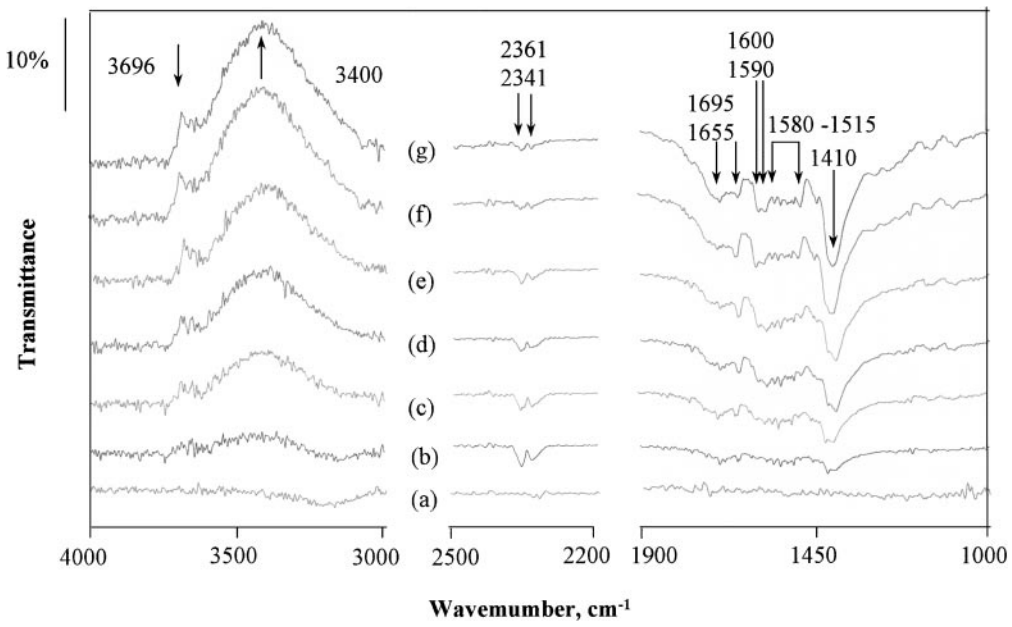

FIG. 6. Time evolution of the infrared spectra of titanium dioxide during *o*-xylene photocatalytic oxidation: (a) prior to lamp illumination ($t = 0$), (b) 0–15 min, (c) 15–30 min, (d) 30–45 min, (e) 45–60 min, (f) 105–120 min, (g) 165–180 min. All spectra are ratioed to titanium dioxide exposed to flowing pure humid air in the dark. Relative humidity equal to 20%.

at 3696 cm^{-1} corresponds to isolated hydroxyls (23). With the ratioing procedure followed, the upward orientations of these peaks indicate consumption and/or desorption of the surface-bound water and hydroxyls.

Major new infrared bands appear in the 1400 to 1800 cm^{-1} range. The two bands appearing at 1695 and 1655 cm^{-1} are characteristic of carbonyl stretches of aldehydes and acids, respectively (24). At short reaction times, bands of approximately equal intensity are observed. With continued irradiation, the 1655 cm^{-1} band becomes more prominent until the end of the third hour on stream. Overlapping bands in the 1515 to 1580 cm^{-1} range accompany the evolution of the carbonyl bands. The bands in this region are indicative of C=C stretch vibrations of an aromatic ring (23). Therefore, the evidence suggests that *o*-xylene is photocatalytically oxidized to aromatic aldehydes and acids in the initial oxidative attack.

In an infrared study of toluene and *o*-xylene thermal catalytic oxidation, van Hengstum (25) assigned bands at 1691, 1651, 1500, and 1410 cm^{-1} to adsorbed *o*-tolualdehyde. In

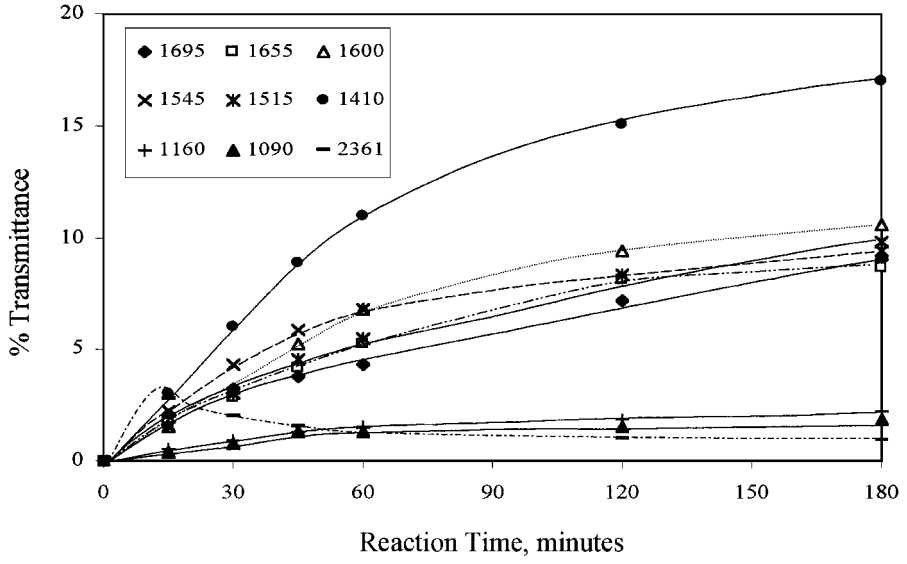

FIG. 7. Time evolution of the intensities of the principal transmittance infrared peaks during *o*-xylene photocatalytic oxidation.

TABLE 1

Assignment of the Observed Infrared Absorption Bands

Compound	Observed bands
o-Xylene	1410 (vs), 1600
o-Tolualdehyde	1695 (s), 1515 (s), 1410
o-Toluic acid	1655 (s)
Benzoate ion	1545 (s)

our experiments the bands at 1695 and 1515 cm^{-1} follow identical time evolution trends and are assigned to *o*-tolualdehyde. Carbonyl bands for acids are observed at lower frequency than corresponding aldehydes; therefore, the 1655 cm^{-1} band is assigned to *o*-toluic acid. The 1545 cm^{-1} band is assigned to asymmetric and symmetric vibration of the benzoate ion, because it is very close to the free ion value of 1548 cm^{-1} (25).

The most prominent band appears at ~1410 cm^{-1}. This band continually increases in intensity with reaction time, at a rapid rate during the first hour on stream and at a gradually declining rate after that time. Another band at 1600 cm^{-1} follows an identical time evolution trend. We believe that these two bands are from the same compound and assign them to adsorbed *o*-xylene. It is probable that a portion of the intensity of the band at 1410 cm^{-1} originates from *o*-tolualdehyde. Liquid phase spectra of *o*-xylene show prominent bands at 1620 and 1445 cm^{-1} due to C–C aromatic ring stretching vibrations (23). These bands are expected to shift down in frequency upon adsorption of *o*-xylene due to interaction with the titania surface. Shifts of similar magnitude have been previously reported for IR bands associated with nonaromatic compounds on photocatalytically active titania (22). In addition, van Hengstum *et al*. (25) observed bands at 1408 and 1600 cm^{-1} in the selective oxidation of *o*-xylene over a vanadium oxide/titanium dioxide catalyst and assigned them to adsorbed *o*-xylene.

It was observed that the reaction rate could be sustained during fixed bed experiments under conditions of high relative humidity and low VOC concentration. In order to understand this phenomenon we conducted two infrared runs: one at 20% relative humidity and the other at 80% relative humidity, while fixing *o*-xylene feed concentration at 50 ppm_v and residence time at 2 s. Figure 8 shows the spectra collected at the end of the third hour on stream for both experiments. These two spectra clearly demonstrate that the surface is covered with significantly more acid (1655 cm^{-1}) and *o*-xylene (1410 and 1600 cm^{-1}) during conditions of low relative humidity. It is interesting to note that the coverage by carbon dioxide is also significantly lower under the low RH condition.

Infrared spectroscopy during regeneration of the catalyst. Regeneration of the catalyst following the just described 20 and 80% relative humidity runs was attempted by shutting down the *o*-xylene flow to the reactor, while flow of humid air maintained at 20 and 80%, respectively, and UV irradiation of the catalyst surface continued. Figure 9 shows the spectra collected during the regeneration of the catalyst deactivated at 20% RH. Figure 9a is the spectrum of the deactivated catalyst surface before regeneration started, while Figs. 9b, 9c, and 9d are spectra of the titania surface after regeneration for 12, 36, and 90 h, respectively. To clarify the nature of the time-evolution of the infrared spectra during regeneration, the peak intensities are tracked and are plotted versus time in Fig. 10. As regeneration proceeds, infrared band intensities universally decrease in intensity, although all the band intensities do not decrease at the same rate. The figure reveals that the intensities of the 1410 and 1600 cm^{-1} bands assigned to adsorbed *o*-xylene reduce at a higher rate in the initial phase of the regeneration compared to the intensities of the other bands. Our earlier assumption that these two bands correspond to the same compound is further justified here by the observation that these two bands exhibit the same time-dependent behavior. With further continuing regeneration, the intensity of these two bands along with all the other bands is reduced

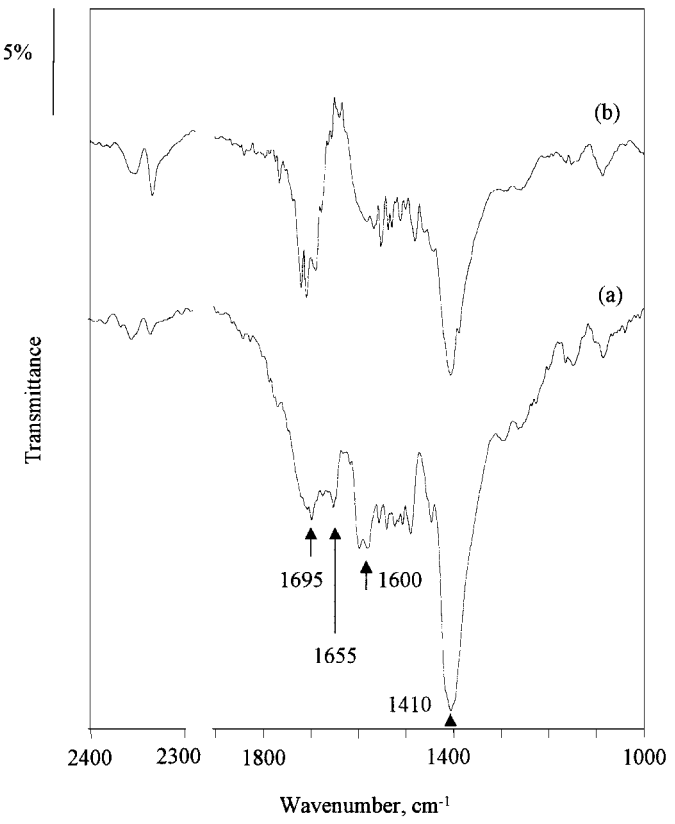

FIG. 8. Transmission infrared spectra of titanium dioxide at the end of third hour during *o*-xylene photocatalytic oxidation as a function of relative humidity in air: (a) 20%, (b) 80%. Spectra shown are ratioed to titanium dioxide exposed to flowing pure humid air in the dark.

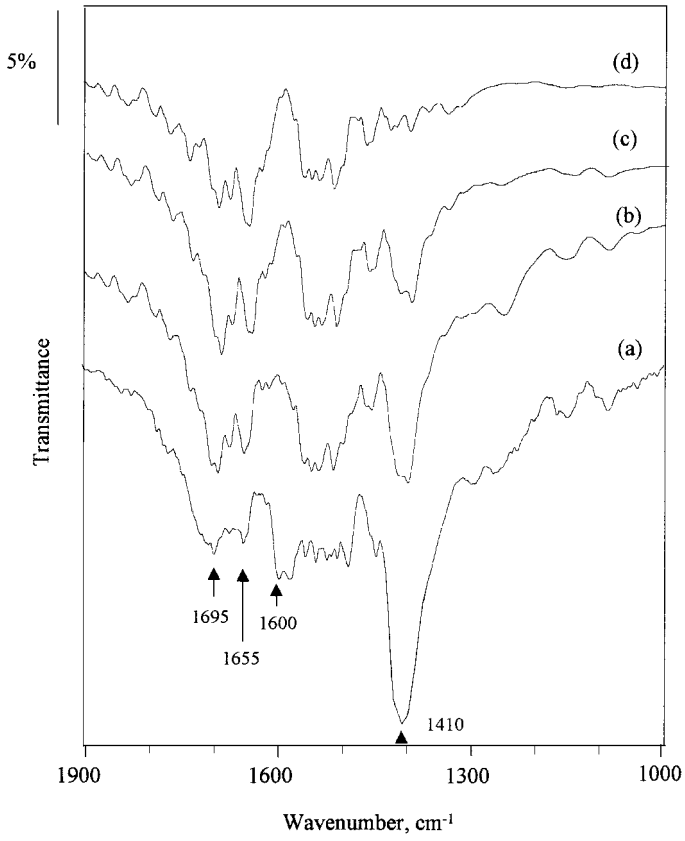

FIG. 9. Transmission infrared spectra of titanium dioxide during regeneration with air containing 20% RH: (a) prior to regeneration, (b) 11–12 h, (c) 35–36 h, and (d) 89–90 h. Spectra shown are ratioed to titanium dioxide exposed to flowing pure humid air in the dark.

at approximately the same rate. The regeneration process was continued for more than 90 h. Even after this lengthy treatment process, a significant portion of the adsorbed intermediates remained.

Figure 11 shows the spectra during the regeneration process of the catalyst surface previously deactivated during PCO with 80% RH air contaminated with 50 ppm_v *o*-xylene. The spectra in Fig. 11a show the infrared bands of the catalyst surface before regeneration, while Figs. 11b and 11c were collected after 6 and 18 h of regeneration, respectively. Figure 12 summarizes the time evolution of the principal infrared bands during regeneration under the conditions of Fig. 11. During the initial regeneration process, the intensities of the bands attributed to *o*-xylene (1410 and 1600 cm^{-1}) decrease more rapidly than the intensities of the other bands. This behavior is similar to that observed for the low humidity case. Unlike the 20% RH case, however, this regeneration scheme resulted in a titania surface free of any adsorbed species in less than 18 h, as indicated by the infrared spectrum devoid of hydrocarbon infrared absorption bands.

DISCUSSION

Fixed bed and infrared experiments yield results that give insight into the photocatalytic oxidation mechanism of dilute *o*-xylene in air and the accompanying catalyst deactivation mechanism. Fixed bed experiments reveal the functional form of the deactivation rate and the dependence of deactivation rate on process parameters. Infrared experiments provide clues to the chemical nature of reaction

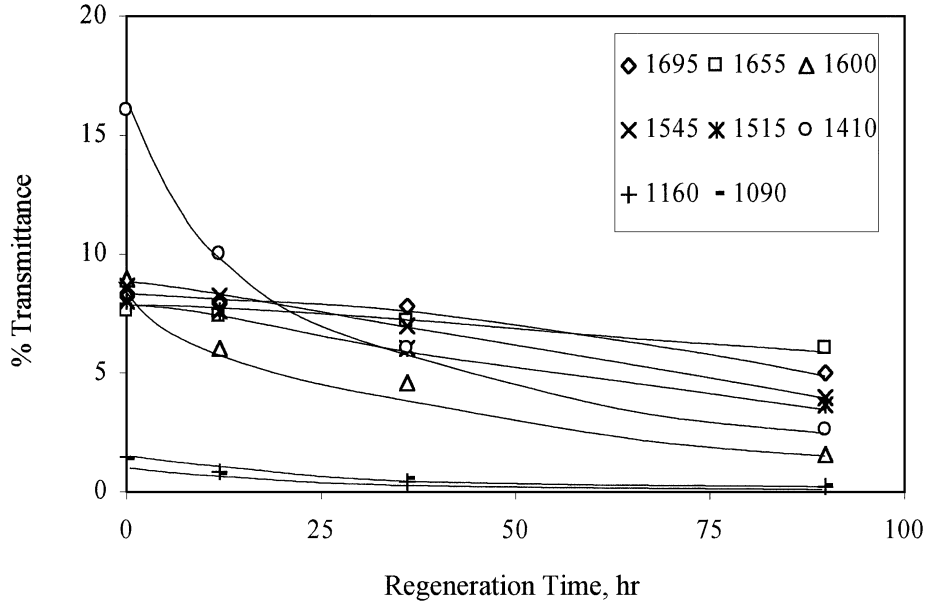

FIG. 10. Time evolution of the intensities of the principal transmission infrared peaks during regeneration of the catalyst. Relative humidity equal to 20%.

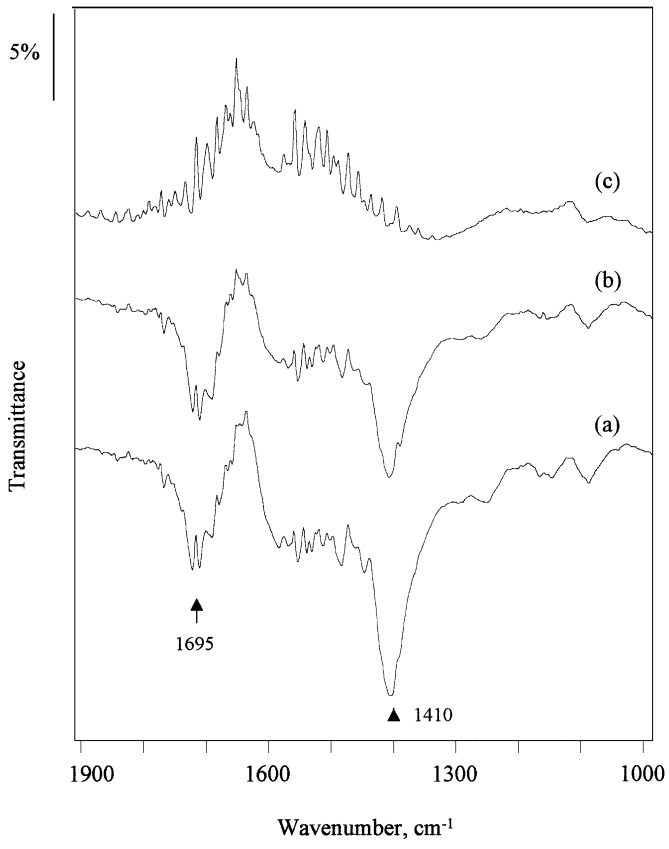

FIG. 11. Transmission infrared spectra of titanium dioxide during regeneration with air containing 80% RH: (a) prior to regeneration ($t = 0$), (b) 5–6 h, (c) 17–18 h. Spectra shown are ratioed to titanium dioxide exposed to flowing pure humid air in the dark.

intermediates and the relative surface coverages by the parent VOC, partial oxidation intermediates, and the complete oxidation products.

The dependencies of deactivation rate on *o*-xylene concentration and relative humidity suggest that experiments can be conducted with very little or no deactivation of the catalyst provided the concentration of *o*-xylene is low and the relative humidity is high. We did not observe deactivation during PCO with air contaminated by 25 ppm_v *o*-xylene and relative humidity of 80% or more. Increasing contaminant concentration or decreasing water vapor concentration favor photocatalyst deactivation.

The empirical exponential decay of the deactivation rate is consistent with a self-poisoning deactivation mechanism in which the deactivating species poisons not only the main reaction, but also the deactivation reaction(s). In this regard, we note that photocatalytic oxidation of aromatic organics proceeds at markedly slower rates than those for nonaromatic contaminants (17). The slower rate is probably caused by the difficulty of breaking the aromatic ring. It is therefore logical to conclude that the reversible deactivation observed here is due to a self-poisoning effect, where the relatively unreactive *o*-xylene and/or a recalcitrant partial oxidation intermediate buildup on the surface, blocking sites that otherwise would serve as centers for reactive species generation. At lower contaminant concentration and higher water vapor concentration, the water vapor can more effectively compete for the active sites, and thus a greater fraction of the active sites are kept clean of carbonaceous compounds. In addition, higher water vapor concentrations favor higher production rate of reactive hydroxyl

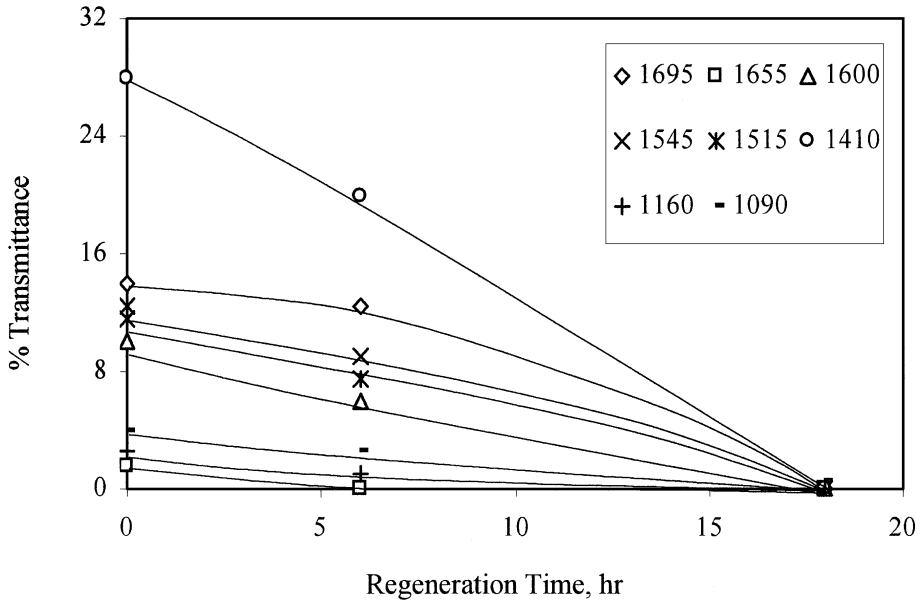

FIG. 12. Time evolution of the intensities of the principal transmission infrared peaks during regeneration of the catalyst. Relative humidity equal to 80%.

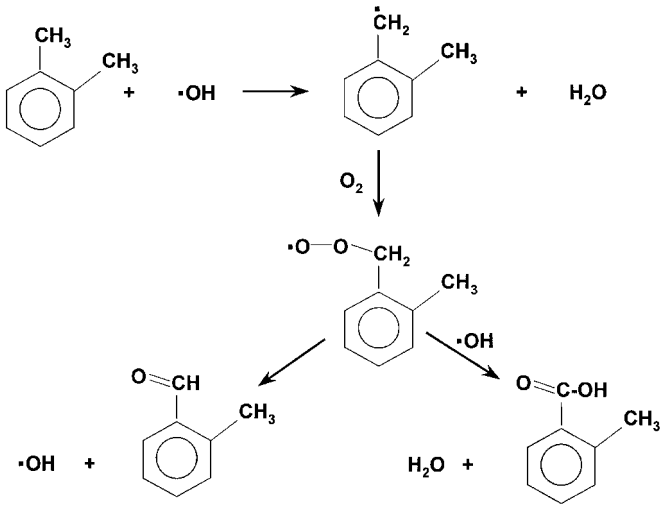

FIG. 13. Proposed mechanism for *o*-toluic acid and *o*-tolualdehyde formation during *o*-xylene photocatalytic oxidation.

radicals, which serve to attack adsorbed reactant molecules and partial oxidation intermediates, thereby decreasing the surface coverages by these compounds.

The presence of strong carbonyl bands in the *in situ* infrared spectra indicates the presence of aromatic aldehydes and acids on the catalyst surface. The most likely candidate partial oxidation intermediates are *o*-tolualdehyde and *o*-toluic acid. Figure 13 illustrates a plausible photocatalytic reaction mechanism that would produce these intermediates if they are indeed formed (recall that infrared band assignments discussed above are yet to be confirmed). Adsorbed *o*-xylene is initially attacked by a hydroxyl radical produced through photoexcitation of the hydroxylated titania surface. The hydroxyl abstracts a hydrogen atom from one of the methyl groups attached to the aromatic ring. Adsorbed oxygen adds at the radical site to produce a reactive peroxy radical, which can rearrange to form adsorbed *o*-toluic acid or decompose to form *o*-tolualdehyde.

Although the deactivation kinetics experiments and *in situ* infrared experiments clearly show that reversible deactivation occurs because recalcitrant partial oxidation products block active catalyst sites, the identity of the specific intermediate responsible for deactivation cannot be unequivocally determined. Under low relative humidity conditions, the titania surface is covered with greater amounts of both *o*-xylene and toluic acid relative to high RH conditions. Although the parent reactant *o*-xylene is present in significant amounts under all process conditions, the fact that there is in addition a significant inventory of partial oxidation products suggests that *o*-xylene oxidation to partial oxidation intermediates is not the rate-limiting step for the complete oxidation process. Instead, it is more likely that the slow oxidation of and the gradual buildup of nonvolatile toluic acid (and/or other aromatic compounds) is responsible for the apparent deactivation of the catalyst.

This hypothesis is supported by the regeneration behavior, in which the partially deactivated surface was restored to its original hydrocarbon free state by treatment in flowing humid air and UV irradiation. In this treatment process, adsorbed organic species were oxidized completely to carbon dioxide. No desorption of *o*-xylene or other VOCs was detected; only CO_2 was evolved from the catalyst surface. Disappearance of *o*-xylene occurred preferentially in the initial stages of regeneration, with oxidation of the tolualdehyde and toluic acid intermediates occurring at a measurably slower rate.

It appears that the role of water vapor is significant in inhibiting deactivation and in regenerating the catalyst. In deactivation inhibition, water vapor limits the self-poisoning nature of aromatic photocatalytic oxidation by effectively competing with the aromatics for active sites (26). However, the fact that water vapor is instrumental in the regeneration process suggests that site competition is not the only phenomenon contributing to deactivation inhibition. Specifically, the regeneration results show that water vapor is critical to oxidation of adsorbed organic species. Adsorbed water can be converted to reactive hydroxyl radicals during photoactivation of the semiconducting titania catalyst. With higher water vapor concentrations, higher concentrations of hydroxyls are produced on the surface, leading to greater scavenging of adsorbed organic intermediates and reduced buildup of recalcitrant compounds.

CONCLUSIONS

Fixed bed deactivation kinetics experiments and *in situ* transmission infrared experiments during photocatalytic oxidation of dilute *o*-xylene provide valuable insight into the reversible deactivation of the gas–solid heterogeneous photocatalytic oxidation process. The reaction rate and the performance of the catalyst (deactivation) are dependent on the *o*-xylene and water vapor concentration. The catalyst deactivates under certain situations. However, low organic concentration (25 ppm_v) and high relative humidity (>80%) lead to steady conversion and no deactivation was detected under these conditions. Deactivation kinetics follow an exponential decay factor form, suggesting a self-poisoning deactivation mechanism. The deactivation parameter α decreases with decreasing organic concentration and increasing relative humidity. Attempts to regenerate the deactivated catalyst by passing zero grade humid air with continued UV irradiation were successful. Infrared spectroscopy during photocatalytic oxidation indicates the presence of significant amounts of *o*-xylene, *o*-tolualdehyde, *o*-toluic acid, benzoate ion, and a small amount of carbon dioxide adsorbed on the catalyst. Low moisture content in the reactant stream favors the accumulation of adsorbed intermediates, especially *o*-xylene and *o*-toluic acid. The apparent loss of activity may be due to

these adsorbed species. Infrared spectroscopy during oxidation and regeneration process also suggests that hydroxyls and/or water play important roles in the overall photocatalytic oxidation process.

ACKNOWLEDGMENTS

This work was supported by United States Environmental Protection Agency (US EPA)-Office of Exploratory Research.

REFERENCES

1. Dibble, L. A., and Raupp, G. B., *Catal. Lett.* **4**, 345 (1990).
2. Dibble, L. A., Ph.D. dissertation, Arizona State Univ., 1989.
3. Dibble, L. A., and Raupp, G. B., *Environ. Sci. Technol.* **26**, 492 (1992).
4. Phillips, L. A., and Raupp, G. B., *J. Mol. Catal.* **77**, 297 (1992).
5. Raupp, G. B., and Junio, C. T., *Appl. Surf. Sci.* **72**, 321 (1993).
6. Raupp, G. B., *J. Vac. Sci. Technol. B* **13**(4), 1883 (1995).
7. Peral, J., and Ollis, D. F., *J. Catal.* **136**, 554 (1992).
8. Sauer, M. L., and Ollis, D. F., *J. Catal.* **149**, 81 (1994).
9. Sauer, M. L., and Ollis, D. F., *J. Catal.* **158**, 570 (1996).
10. Raupp, G. B., Nico, J. A., Annangi, S., Changrani, R., and Annapragada, R., *AIChE J.* **43**, 792 (1997).
11. Nimlos, M. R., Jacoby, W. A., Blake, D. M., and Milne, T. A., *Environ. Sci. Technol.* **27**, 732 (1993).
12. Jacoby, W. A., Nimlos, M. R., Blake, D. M., Noble, R. D., and Koval, C. A., *Environ. Sci. Technol.* **28**, 1661 (1994).
13. Jacoby, W. A., Blake, D. M., Noble, R. D., and Koval, C. A., *J. Catal.* **157**, 87 (1995).
14. Peral, J., and Ollis, D. F., "The First International Conference on TiO_2 Photocatalytic Purification and Treatment of Water and Air, London, Ontario, Canada," p. 741. Elsevier, Amsterdam/New York, 1993.
15. Cunningham, J., and Hodnett, B. K., *J. Chem. Soc. Faraday Trans. 1* **77**, 2777 (1981).
16. Blake, N. R., and Griffin, G. L., *J. Phys. Chem.* **92**(20), 5697 (1988).
17. Kalaga, M., M.S. thesis, Arizona State Univ., 1998.
18. Jacoby, W. A., Blake, D. M., Fennell, J. A., Boulter, J. E., Vargo, L. M., George, M. C., and Dolberg, S. K., *Air Water Manage. Assoc.* **46**, 891 (1996).
19. Sauer, M. L., Hale, M. A., and Ollis, D. F., *J. Photochem. Photobiol. A* **88**, 169 (1995).
20. Luo, Y., and Ollis, D. F., *J. Catal.* **163**, 1 (1996).
21. Raupp, G. B., "Final Contract Report: Photocatalytic Oxidation for Point-of-Use Abatement," Semiconductor Research Corporation Report 21170, 1996.
22. Ameen, Md. M., Ph.D. dissertation, Arizona State Univ., 1998.
23. Little, L., "Infrared Spectra of Adsorbed Species." Academic Press, London, 1966.
24. Pouchert, C. J., "Aldrich Library of Infrared Spectra." Aldrich, Milwaukee, WI, 1981.
25. van Hengstum, A. J., Pranger, J., van Hengstum-Nijhuis, S. M., van Ommen, J. G., and Gellings, P. J., *J. Catal.* **101**, 323 (1986).
26. Obee, T. N., and Brown, R. T., *Environ. Sci. Technol.* **29**, 1223 (1995).